The Influence of Ink and Paper on Bar Code Print Quality and Readability with OCR Scanning Systems

Judith Auslander, Mike Chen, Robert Cordery, and Claude Zeller, Pitney Bowes Inc., Shelton, Connecticut, USA;
Ming-Kai Tse, QEA,, Burlington, MA, USA

Abstract

Postal operators worldwide use two-dimensional Data Matrix bar codes for machine-readable postage payment evidencing. Dynamic interaction of ink jet inks with uncontrolled media like envelope papers generates a variety of print quality defects. Adaptive thresholding algorithms optimized for OCR amplify the impact of these defects on the readability of two-dimensional bar codes. Print quality parameters are determined according to international standards for several combinations of monochrome franking ink jet inks and plain paper envelopes. The ink and paper characteristics relevant in generating the defects are measured and interpreted in terms of wetting and capillarity. We investigate, through computer simulation, the impact of the interaction of print quality defects and OCR adaptive thresholding algorithms on 2D bar code readability.

The Challenge

Several posts have introduced postage evidencing systems using a Digital Postage Mark (DPM) containing machine-readable information printed on the upper right corner of a mail piece. Posts need to reliably read the DPM printed by the mailer as postage payment evidence. Readability becomes a "must" for service reliability with the inclusion of track-and-trace, delivery confirmation and other value-added services in the DPM. United States Postal Service (USPS), Deutsche Post, Swiss Post and others have implemented systems that use a two-dimensional bar code symbol in the DPM. Others such as France's La Poste use optical character recognition (OCR) symbology. Posts and meter manufacturers jointly face the challenge of achieving highly reliable machine reading of the DPM.

There are barriers to achieving the necessary read rates throughout the DPM printing and scanning process. These barriers are divided into three categories. properties of the printed image; noise added to the image by mail piece handling; and properties of the scanned image. Here we focus on the printing and scanning categories.

Digital Postage Marks are often printed by drop-on-demand ink jet at high speed, resulting in printer specific defects such as satellites, dot placement errors and misfiring nozzles. The use of uncontrolled envelope media further reduces print quality. Mailers select envelopes with a broad range of reflectance resulting in a wide range of print contrast. The interaction between the paper and ink contributes to a range of print quality defects including print growth, mottle, graininess, edge raggedness and blurriness as defined in International Standard ISO/IEC 13660.[13]

Postal scanners are designed to operate efficiently in postal sorters and other automation equipment. Sorters divide an input mailstream into multiple output channels based on information in the address. The sorter may operate at a speed of 10 mail pieces per second or higher. Imaging systems operating at such high speeds invariably introduce noise. Manufacturers of postal automation equipment have developed sophisticated scanning systems able to accurately recognize addresses with low print quality and low contrast on dark envelopes.

High-speed recognition systems, such as those implemented in sorters, usually operate on binary thresholded images simply to reduce the amount of information communicated and processed. Although the thresholding algorithms used in postal sorters are not optimum for two-dimensional bar code scanning, the scanners are being pressed into service as DPM readers. In many cases, thresholding algorithms are implemented in firmware that cannot be easily modified. Postal scanners work very well for their primary sorting function that includes reading linear barcodes such as POSTNET and 4-state symbologies. It is unlikely that they will be modified or reparametrized in the immediate future for reading the two-dimensional bar codes in the DPM.

In section 2 we discuss the print quality standards for the postal application. Section 3 provides an overview of aspects of typical thresholding algorithms used for reading text. Section 4 describes printing and scanning simulation. Section 5 describes experimental results of selected ink and paper properties and print quality measurements. Section 6 describes five cases of ink/paper systems with simulation results.

Print Quality and Digital Postage Mark Standards

The Universal Postal Union (UPU) introduced standards for DPMs with two-dimensional bar codes in UPU standard S-28.[18] Additional UPU standards provide requirements for other features of the DPM including UPU standard S-36[19] and UPU standard S-44-1.[20]

There are a variety of international standards relevant to printing a DPM with a two-dimensional matrix code. ISO/IEC 16022[16] is the international standard for Data Matrix and provides the reference decode algorithm. CEN TS14826/ISO/IEC 18050,[17] defines general print quality and test procedures for DPMs. ISO/IEC 18050 is an application standard that refers for print quality definitions to ISO/IEC 15415.[15]

Symbol quality is critical for readability. Contributors to symbol quality include symbol contrast, modulation, axial non-uniformity, grid non-uniformity, damage to the finder pattern. Here we will address symbol contrast and modulation, which relate most closely to ink and paper characteristics. Grid non-uniformity impacts the ability of the recognition system to find the center of each module. Errors in finding the centers add to the noise in measuring the gray level of each module. The magnitude of this impact depends on the algorithm used to find the centers. Algorithms compliant with the standards must be designed to find the centers of modules at least as well as the method defined in the reference decode algorithm of ISO/IEC 16022, which uses the finder pattern and geometrically divides up the interior of each data region.

The reference decode algorithm in ISO/IEC 16022 first blurs the grayscale image by convolving it with a circular aperture whose diameter is typically 0.8 times the module dimension X. The reflectance R_m for each module m is then measured at the center of the module. Symbol contrast is the difference between the maximum reflectance R_{MAX} and the minimum reflectance R_{MIN}:

$$SC = R_{MAX} - R_{MIN} . \quad (1)$$

The Data Matrix symbol is constructed from groups of eight modules called codewords. Each codeword has a modulation M_{CW} given by:

$$M_{CW} = \frac{\min_{m \in CW}(2 \cdot |R_m - Thresh|)}{SC} \quad (2)$$

where *Thresh* is a global threshold set, for the standard, at (R_{MAX} + R_{MIN})/2. The influence of the set of M_{CW} values on the symbol quality depends on the number of codewords with modulation below certain predetermined values compared to the number of error correction codewords.

Thresholding

Thresholding algorithms produce a binary image with pixel values 0 (black) or 1 (white) from a grayscale image with pixel values ranging between 0 and 1. The selection of the algorithm and optimal setting of parameters depend on the statistical properties of the images being processed and the information being extracted. There are several aspects of typical methods that can be used to categorize thresholding. The method may be local or global.[0] A global method sets a single threshold for the image. The reference decode algorithm sets this threshold at (R_{MAX} + R_{MIN})/2. In a local method, the threshold depends on the local properties of the grayscale image. There are a variety of schemes for setting the local threshold. The reference decode algorithm sets a lower bound for the performance of thresholding algorithms.

Thresholding for postal automation has been subject to intense research interest during the last two decades. As the first step of an entire system for OCR, thresholding is crucial and its success is essential for all further processing. Obtaining a very robust thresholding method depends on tuning the algorithm to the application. Mail moves through typical mail automation equipment at ten mail pieces per second. There are only a few milliseconds for capturing, processing and thresholding the image. To save computing time, thresholding algorithms invariably involve limited or no preprocessing of the gray scale image. Posts have optimized the algorithm to read addresses with poor contrast and print quality. Moreover, the envelope reflectivity may vary across the mail piece. The threshold must therefore adapt to the local gray level of the image.

The local Niblack algorithm sets a threshold T_p for each pixel p as a linear combination of the mean M_p and the standard deviation σ_p of the reflectivity of pixels within a window centered on p.

$$T_p = M_p + k_N \sigma_p , \quad (3)$$

where k_N is a constant, typically around -0.2 for optical character recognition. The negative value thins lines and avoids joining characters. The binary image is assigned the logical value ($R_p < T_p$). The local Niblack thresholding algorithm is a typical example of several local adaptive methods. Many algorithms substitute other values such as (R_{MAX} + R_{MIN})/2 for M_p or values such as (R_{MAX} - R_{MIN}) for σ_p where R_{MAX} and R_{MIN} are determined over the window.

Most fonts used for addresses have character stroke widths on the order of 0.3 mm. The size of the window must be several times the stroke width so that the window includes both printed and unprinted areas. The calculation complexity is proportional to the window area, so typically the window size is set to the minimum acceptable value for the application. For reading characters in an address, a reasonable value for the window dimension is 1 mm. The size of a module in a postage indicium is about twice the typical character stroke width.

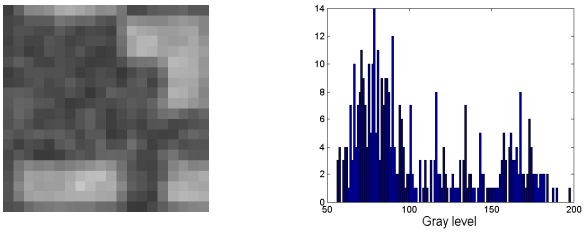

Figure 1. Gray level histogram of portion of a barcode

Although local adaptive algorithms yield considerably better results than global adaptive algorithms,[9] it has been found that local average methods such as Niblack's method,[6] which is often quoted as one of the best adaptive algorithms, tend to break down in the presence of homogeneous print areas larger than the window and hence require post-processing.[10] A portion of a gray scale image of a barcode printed on a rather dark envelope is shown in Figure 1. Thresholding using a local algorithm with a small window results in a poor binary image of the barcode that reduces readability. As shown in Figure 2, the local threshold results in white pixels in dark modules that could be confused with print problems.

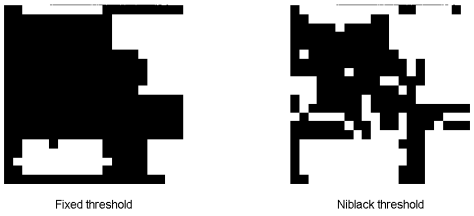

Figure 2. Comparison of fixed and Niblack thresholds

Printing and Scanning Simulation

In order to obtain a repeatable comparison of the effect of print quality on various algorithms for reading Data Matrix barcodes, we simulate the printing, imaging and reading processes. The simulation is intended to capture the basic features of scanned barcodes. It is not a calculation based on first principles. The simulation proceeds with an image produced by convolving the bitmap of a random barcode as sent to the printer with an average printed dot. Noise representative of typical print quality attributes is then added to both the unprinted paper area and to the printed area. Additional noise is added that is typical of high-speed imagers. The resulting image is then processed to obtain a thresholded binary image. The barcode information is extracted and compared to the input data.

The input data is a random array in the form of a Data Matrix bar code. Error-correction coding is irrelevant for our objectives because we want to count the number of modules that are incorrectly read. The objective is to compare input module bit values to output bit values and identify the number and type of errors. Note that the simulated images in this paper will not decode with a standard Data Matrix algorithm because they are not encoded.

Observation of various envelope papers and printed areas leads to the conclusion that the mean square noise spectrum has a self-similar, fractal property. The mean square value of the Fourier coefficients is proportional to a negative power of the magnitude of the wavevector k for reasonably large values of k:

$$\left\langle R_{\vec{k}} R_{-\vec{k}} \right\rangle \sim k^{-2\alpha}, \tag{4}$$

where R_k is a Fourier component of the reflectivity. For plain papers and inks typical of mailing applications, the value of α is approximately 1. The resulting image reproduces the characteristic statistics of scans of paper and ink. The contrast in example noise pattern in Figure 3 has been enhanced to emphasize the geometric distribution of the noise. The three parameters in this model of paper reflectance are the maximum and minimum reflectances of the paper and the exponent α. We use the same model, with different parameters, for ink reflectivity.

The simulation uses a circular parabolic ink distribution for a single drop and models overlap of drops as simply additive. The reflectance is derived from the amount of ink using the Kubelka-Munk[4] transform in the infinite pad approximation. The paper and ink noise models are then used to modify the barcode image.

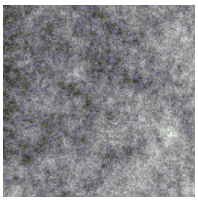

Figure 3. Simulation of paper and ink noise

The scan of the image is simulated by convolution with a linear filter representing one pixel of the scanner at a resolution of 200 dpi. A simple background rejection scheme determines for each scanned pixel whether it is to be interpreted as background. If the pixels in a 3 by 3 square centered on the scanned pixel fall within a print contrast ratio range of 0.15, then the pixel is background. The simulation tests three schemes for processing the image. averaging the gray scale image over an aperture; binarizing the image with an adaptive algorithm using a small 7 by 7 scanner pixel window; and finally binarizing the image with an adaptive algorithm using a larger 15 by 15 scanner pixel window.

Selected Ink and Envelope Paper Properties and Print Quality Attributes

The printing of high-density 2D bar codes by ink jet printers involves the three system components. printer, ink, and substrate. Dynamic interaction of ink jet inks with uncontrolled media like envelope papers generates a variety of print quality defects. Here we discuss ink and substrate and more specifically the print quality resulting from spreading and penetration of water-based inks on envelope paper.

Experimental Data

We generated DPM DataMatrix bar code prints using three digital postage meter printers. The resolutions of these printers are 400x600dpi, 300x600dpi, and 300x600dpi respectively. We used four different monochrome blue inks designed to meet postal specifications. We printed on seventeen different envelopes with a variety of reflectance spectra, porosity, roughness, hydrophilicity, pH, and surface energy.

1. Envelopes were conditioned at 23°C and 50% RH before testing.
2. TMI Monitor Smoothness Model 58-02 machine was used for smoothness and porosity measurements.
3. The minimum value of porosity is 36 SU for this instrument.
4. Cobb sizing test was performed according to TAPPI 441 om-98 using a Gurley Precision Instrument.

As we may see from this table the set of envelopes is diverse covering a broad range of porosity, some variation in roughness and polarity as measured by Sheffield porosity, Sheffield smoothness and by Cobb sizing. The coated envelope No. 5 is most hydrophilic.

Table 1: Properties of Envelopes

Envelope Number	Porosity (Sheffield)	Smoothness (Sheffield)	Cobb Sizing (g/m^2)	pH
1	164	143.4	30	7.97
2	98.8	254.1	22	7.26
3	125	228.4	24	7.31
4	36	19.3	51	8.71
5	36	84.5	82	8.86
6	94.0	182.8	32	7.49
7	94.1	179.2	28	7.55
8	149.0	163.4	22	8.09
9	161.1	136.7	20	7.89
10	135.3	161.6	22	7.85
11	110.5	159.6	24	7.86
12	115.6	136.5	22	8.12
13	36	145.2	31	6.67
14	36	189.9	33	6.38
15	36	171.4	32	5.62
16	36	175.5	33	6.85
17	36	176.6	31	6.48

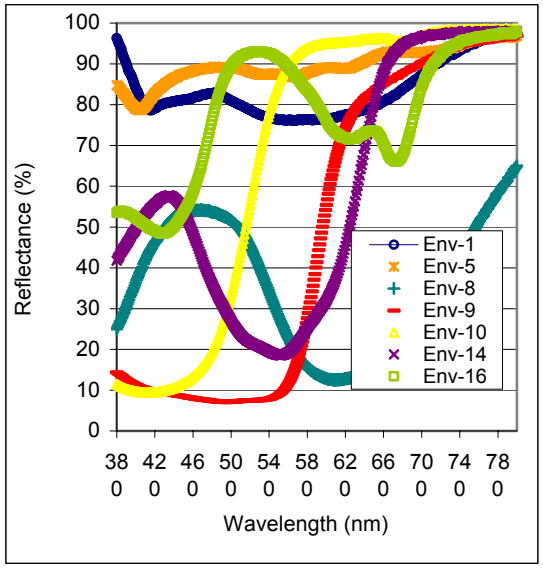

Figure 4. Reflectance spectra for selected envelopes

Figure 4 shows that some envelopes can have a reflectance spectrum similar to the ink therefore resulting in low contrast.

Ink

The measured ink characteristics are viscosity, surface tension, viscosity variation with shear rate, reflectance, contact angle, and contact angle variation with time.

The surface tension varied from 28 dynes/cm for ink 4 to 40.2 dynes/ cm for ink 2 which will influence the capillary spreading according to Lucas Washburn.

Table 2: Properties of Four Blue Inks

Ink ID	Viscosity (cp)	Surface Tension (dyne/cm)	pH
Ink #1	2.02	33.7	7.32
Ink #2	2.06	40.2	6.69
Ink #3	2.32	32.8	6.95
Ink #4	3.32	28.0	8.07

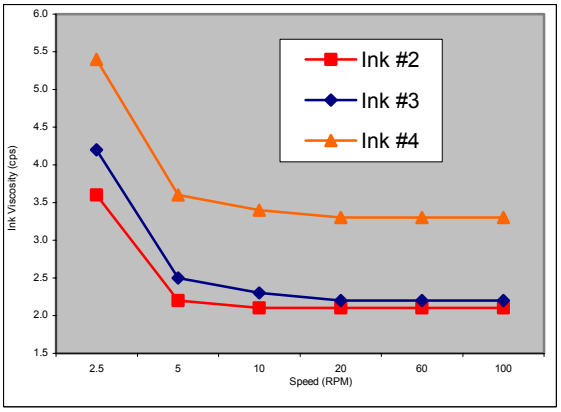

Figure 5. Dynamic ink viscosity

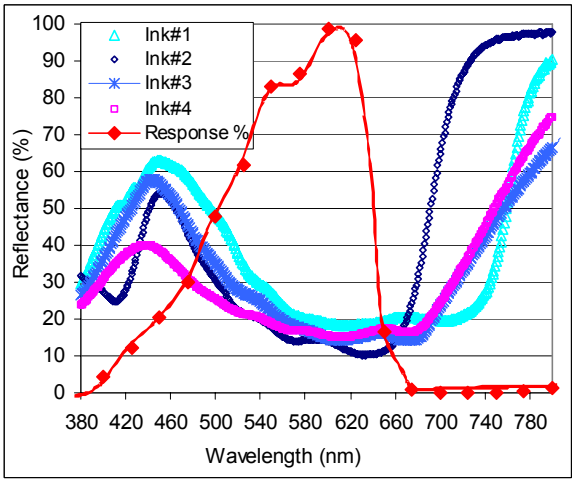

Figure 6. Reflectance spectra for prints with the 4 inks and the spectral response of a scanner.

The viscosity dependence on shear rate shown in Figure 5 was measured with a Brookfield viscometer with a low viscosity fluid probe. We can see noticeable differences in the viscosity at low shear rate. Inks 3 and 4 show higher viscosity at low shear rate, which may explain differences in the contact angle and its variation with time.

All the inks were dark blue according to the new postal ink specifications in some European countries. The reflectance spectra of these 4 inks on a white envelope can be seen in the Figure 6. The typical spectral response of a scanner is represented in order to define the spectral region of interest for maximum contrast.

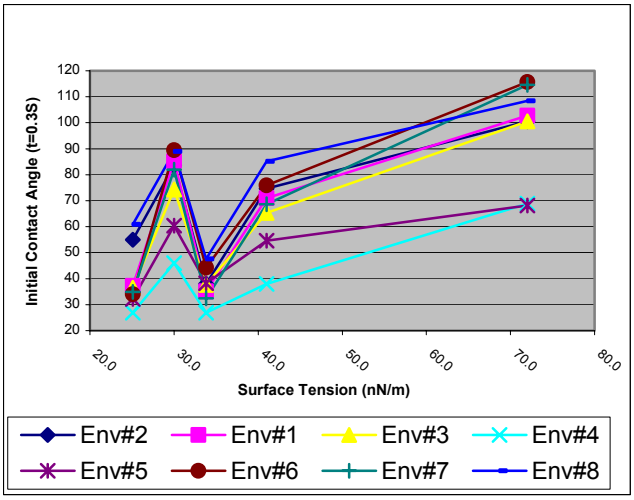

Figure 7. Surface Tension for Inks vs. Contact Angle on Envelopes #1 to #8

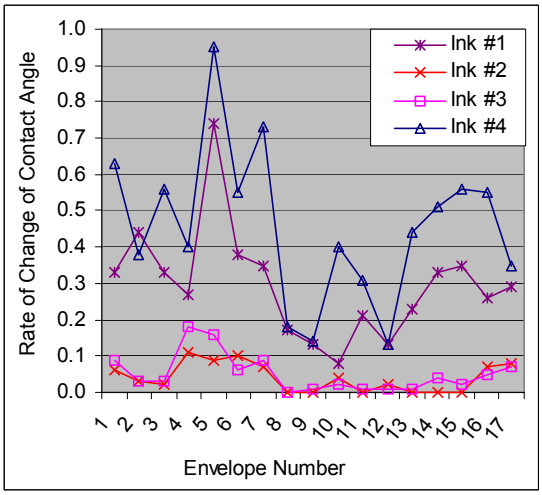

Figure 9. Rate of change of contact angle for inks on different envelopes

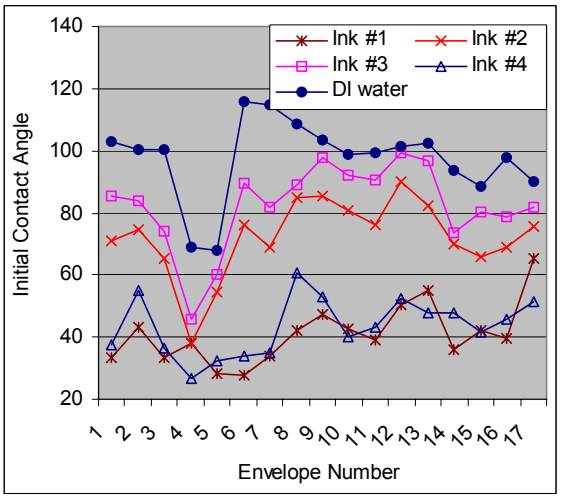

Figure 8. Initial contact angle for inks and DI water on different envelopes

Figure 7 shows the dependence of the contact angle on the surface tension for the four inks on selected envelopes. We can see that ink 3 shows a deviation from the linear dependence of the contact angle θ on the surface tension γ according to Young equation. This may explain some differences in print quality attributes such as mottle and print growth which are shown later in the paper.

Figure 8 gives us an indication of the surface energy of the envelopes. For example the envelope 5, which is the most hydrophilic, shows the lowest contact angle.

Figure 8 describes the dependence of the contact angle of the four inks on the type of envelope and Figure 9 shows its variation with time. The rate of change of contact angle can predict ink spreading. For example, print growth is high for ink 1, which has the highest rate of change of contact angle While inks 3 and 4 had low print growth.

Ink-Paper Interaction

Ink-paper interaction generates noise due to variations in the paper surface characteristics and to its interaction with inks with various surface and viscoelastic characteristics.

The degree of ink spreading and penetration depends on several ink parameters such as viscosity, surface tension, and contact angle as well as paper parameters such as surface chemistry, roughness and porosity.

The equilibrium of wetting properties of liquids on ideal surfaces can be described by the Young equation.

$$\gamma_{sv} - \gamma_{sl} = \gamma_{lv} \cos\theta \qquad (5)$$

containing the interfacial tensions on the triple phase contact line. θ is the contact angle, the subscripts *lv*, *sl* and *sv* describe the liquid-vapor, solid-liquid and solid-vapor interfaces.

The capillary spreading on porous media is described by the Lucas Washburn equation[11] for the rate of penetration of fluid in a capillary of radius *r*:

$$dh/dt = (r\,\gamma_L \cos\theta)/(4\eta h) \qquad (6)$$

where h is the length of filled portion of the capillary, η is the fluid viscosity of the liquid, γ_L is the surface energy of the liquid, and θ is the contact angle.

These equations are an oversimplification since the paper is not a straight capillary tube but a network of fibers. The contact angle depends on other properties such as penetration, porosity, pore size and surface energy. Wetting is enhanced by rough surfaces for liquids with contact angles less than 90 degrees and is inhibited for liquids with higher contact angles.[2]

Print Quality Analysis

We measure print quality parameters (contrast, print growth, mottle and graininess) as defined by ISO 13660 with a QEA Personal Image Analysis System IAS. The measurements were made in the red channel corresponding to the peak of the scanner response.

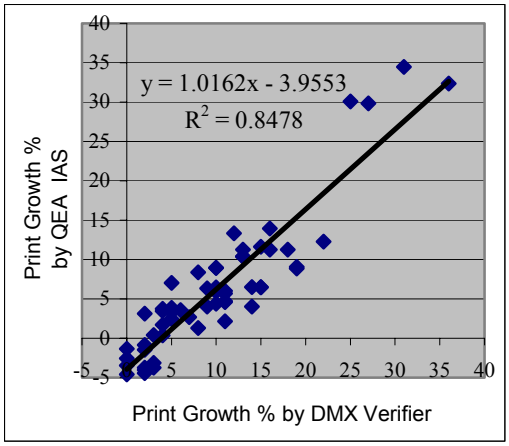

Figure 10. Correlation between IAS and Verifier for measurement of print growth

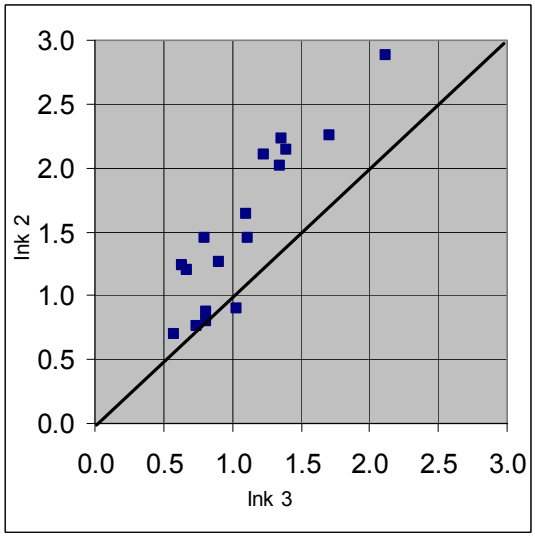

Figure 11. Mottle for inks #2 and #3

The print growth was measured with an Acuity CI Matrix DMx Verifier for Data Matrix symbology. This method can give a more direct correlation with readability. We found a very good correlation between the two methods of measuring line quality, as expected.

Figure 11 compares the mottle for two inks on the seventeen envelopes.

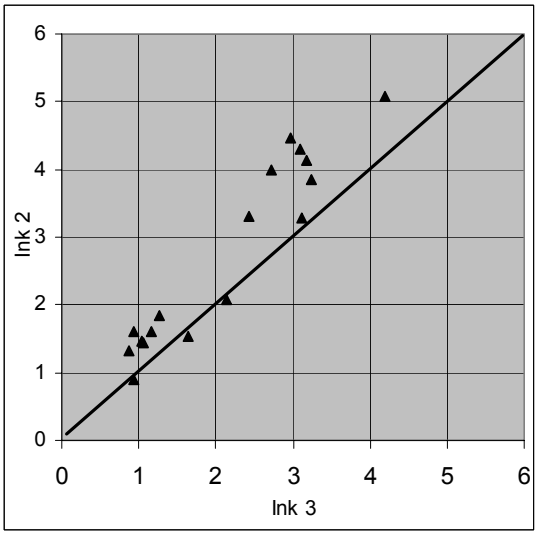

Figure 12. Graininess for inks #2 and #3

The non-uniformity of coverage defined by ISO 13660 as mottle and graininess is given only for inks 2 and 3. From both measurements we can see that ink 2 shows less uniform coverage than ink 3. From the fluid properties we could interpret it as a result of higher tendency to coalescence due to lower viscosity at low shear rate. More measurements are needed in order to confirm this effect. If the ink can be designed to show some non-Newtonian behavior as shown in Figure 5 this might help control in the future the coverage of rough substrates.

Results for the Five Cases

From the experimental data on several inks and envelope papers we devised scenario of ink/paper interaction in order to gain understanding of the range of effects produced. We describe several cases of defects generated by specific ink/paper characteristics that are important for machine readability of 2D bar codes. These include spreading and non-spreading inks combined with porous, non-porous, hydrophilic, rough and smooth papers.

The ink/paper defects such as print growth, non-uniform ink coverage (graininess, mottle) which cause low modulation can have a detrimental influence on readability.

We describe several cases of spreading behavior of water-based inks on a range of substrates. Five illustrative examples of ink/paper systems are described. The role of the different factors such as surface tension, surface roughness and porosity, contact angle influencing the spreading behavior is discussed.

This is the ideal case where the ink characteristics are optimized for the paper and the image is as close as possible to the bitmap image of the bar code. The fluid viscosity and surface tension are characteristic values for thermal ink jet: $\eta = 1.5–3$ cps, $\gamma = 33–37$ dynes/cm. The surface coating of the paper is optimized for high quality printing with water based inks such as for example photo quality paper with controlled particle size and surface properties coating.

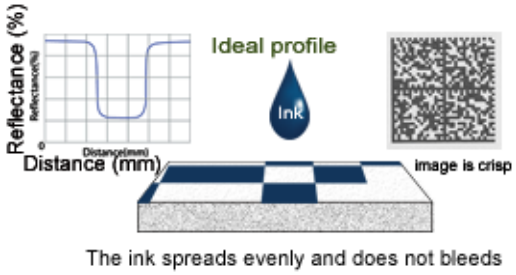

Figure 13. Case 1 – Non-wetting ink on smooth, low porosity paper

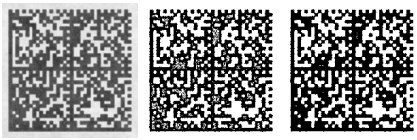

Figure 14. (Case 1) Non-wetting ink on smooth low porosity paper (ideal profile)

The reflectance profile varying from the maximum value for the substrate to the minimum value for the printed symbol is as close as possible to the bitmap image.

The "ideal profile" case shown in Figure 14 has high print quality. The percentage of codewords incorrectly interpreted for the three cases are.

Gray scale threshold.	0.0%;
Small binarizing window	9.2%;
Large binarizing window	0.2%

Note that even for this ideal case, the percentage of incorrectly read codewords is precariously close to the limits of the symbol when using a small window. The problem is that modules tend to be hollowed out by the thresholding process.

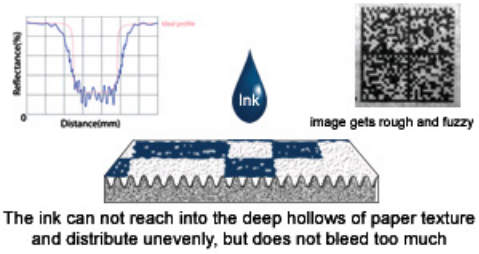

Figure 15. Case 2 – Wetting ink on white, rough, high porosity paper

This case describes the interaction between a low surface tension, low contact angle ink with a rough, high porosity paper. The ink does not saturate the paper due to higher void volume but produces irregular edges and does not spread uniformly. Therefore the edges show feathering effects and there is a considerable variation in optical density with low percentage fill of the symbol. The reflectance profile is noisy with microscopic variation in minimum reflectance due to paper microstructure variation.

Figure 16. (Case 2) Wetting ink on rough high porosity white paper

Gray scale threshold.	0.0%;
Small binarizing window	7.2%;
Large binarizing window	0.0%

The three preprocessing algorithms in this case performed essentially the same as in they did in Case 1.

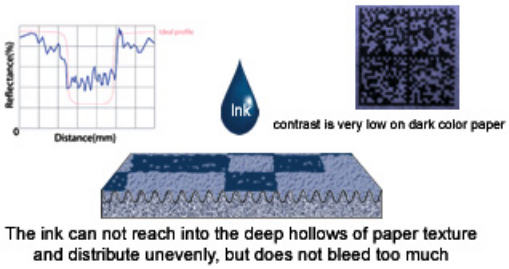

Figure 17. Case 3 – Wetting ink on dark, rough, high porosity paper

This case is similar to the previous case but here the contrast is much smaller due to the low reflectance of the paper. The reflectance profile shows this clearly by the noisy and small variation of reflectance with distance.

Figure 18. (Case 3) Wetting ink on Dark, Rough high porosity paper

Gray scale threshold.	0.2%;
Small binarizing window	40%;
Large binarizing window	7.3%

In Case 3 shown in Figure 18 even with low contrast, the gray scale thresholding scheme still performs well. Both binarization algorithms had problems with the small window version failing to read the barcode and large window version using up about half the available error correction.

This case describes the interaction between an ink with low surface tension and contact angle that interacts with a high roughness, low porosity paper, for example pergamyn paper (glassinepaper). The ink saturates the limited void volume of the paper surface and bleeds outside the symbol borders also creating void space and irregular coverage of the symbols. This results in bar codes that are not gradable and not readable.

The reflectance profile is very noisy and overflows the bitmap original dimensions.

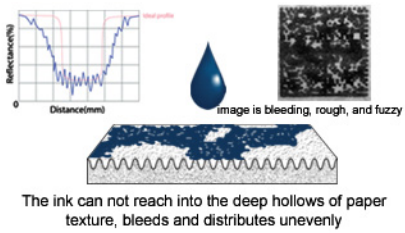

Figure 19. Case 4 – Wetting ink on white, rough, hydrophilic, low porosity paper

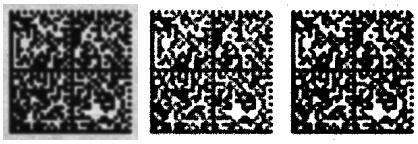

Figure 20. (Case 4) Wetting ink on white, rough, low porosity paper

Gray scale threshold.	1.6%
Small binarizing window	2.5%
Large binarizing window	22%

In the case of excessive print growth shown in Figure 20 the small binarizing window performs reasonably well, but the large binarizing window fails to read. A white module surrounded by dark modules is darkened due to print growth. The large binarizing window often includes a substantial light area, so the threshold will be set quite bright and the module is interpreted as black. The smaller window only includes neighboring dark areas and the relatively lighter area of the subject module.

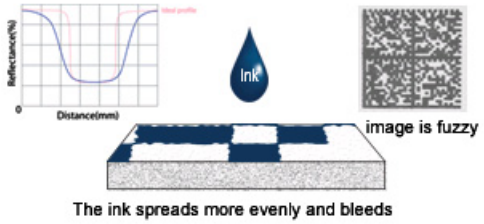

Figure 21. Case 5 – Wetting ink on white, smooth, low porosity, hydrophilic paper

This is a low surface tension, low contact angle ink printed on coated, hydrophilic paper. The ink spreads uniformly and bleeds considerably outside the assigned space on the bar code. The symbol is still readable but the number of errors is high. The reflectance profile is smooth transition but with a very high print growth outside the ideal profile.

Figure 22. (Case 5) Wetting ink on smooth, low porosity paper

Gray scale threshold.	0.0%
Small binarizing window	25.6%
Large binarizing window	0.6%

Here the small binarizing window again fails to read the barcode.

Conclusion

Readability of two-dimensional barcodes is adversely impacted by the properties of legacy binary scanners optimized for sorting mail combined with defects generated by specific ink and paper characteristics.

OCR thresholding algorithms are designed to binarize and segment character images on low reflectance papers. Ink-paper defects such as print growth, graininess and mottle induce a variable modulation that has a detrimental influence when combined with an inadequate thresholding scheme.

All cases with fairly good print quality performed reasonably well with the large binarizing window. A small binarizing window typical to those used in OCR failed in most case. In all cases, the grayscale threshold performed better than either binarizing algorithm. Grayscale scanners, such as the USPS Wide Field of View camera are well suited to reading two-dimensional bar codes.

We discussed in this paper several cases of defects generated by specific ink-paper characteristics, which are important for machine readability of 2D bar codes. These include spreading and non-spreading inks combined with porous, non-porous, hydrophilic, rough and smooth papers. We presented the resulting print quality characteristics. contrast, print growth, mottle, graininess and modulation that can be detrimental to readability.

Postage meter vendors have control over some aspects of DPM production. We provide ink designed to produce DPM bar codes on suitable envelopes that are machine-readable with suitable scanners. Through experiment and modeling we can modify the items under our control to improve readability.

Acknowledgements

We would like to thank Dr. Long Lin from University of Leeds UK for some of the ink measurements and for valuable discussions. We would also like to thank Daisuke Sawaki for artwork. Thanks also to Dr. Ming Kai Tse from QEA, Inc. for Print Quality measurements.

References

1. J. Auslander, D. Mackay, C. Zeller, J. C. Briggs, and M. K. Tse "InkJet Printing for Mailing Application" *IS&T NIP15. International Conference on Digital Printing Technologies*, Oct. 17-22, 1999, PP. 141-148.
2. J. Auslander, R. Cordery, and C. Zeller, "Parameters Influencing Ink/Envelope Interaction and Bristow Absorption" *IS&T NIP13. International Conference on Digital Printing Technologies*, November 2-7, 1997, PP. 450-455.
3. M. von Bahr, F. Tiberg, and B. V. Zhmud "Spreading Dynamics of Surfactant Solutions" *Langmuir*, *Vol. 15, No.20*, 1999, PP 7069-7075.
4. Kubelka and Munk, Zeit. Für Tekn. Physik, 12, p593 (1931).
5. A. Marmur "Wettability Characterization of Printing Substrates. Facts and Interpretations" *IS&T NIP17. International Conference on Digital Printing Technologies*, October 2001; PP. 129-132.
6. W. Niblack. An Introduction to Digital Image Processing. Prentice Hall, Englewood Cliffs, 1986.
7. B. Sankur, M. Sezgin, A Survey Over Image Thresholding Techniques And Quantitative Performance Evaluation, Journal of Electronic Imaging, 13(1), 146-165, January 2004.
8. F. Tiberg, B. V. Zhmud,K. Hallstensson and M. von Bahr "Capillary Rise of Surfactant Solutions" *Phys. Chem. Phys.,* 2000, 2, PP. 5189-5196.
9. Ø. D. Trier and A. K. Jain. Goal-directed evaluation of binarization methods. IEEE Transactions on Pattern Analysis and Machine Intelligence, 17(12).1191–1201, 1995.
10. J. S. Valverde and R. Grigat. Optimal binarisation of technical document images. In ICIP 2000 Proceedings, pages 985–988. IEEE, September 2000.
11. E. W. Washburn, *Phys. Rev.* 2nd Series, 17, 273 (1921).
12. B. Zhmud "Dynamic Aspects of Ink-paper Interaction in Relation to Inkjet Printing" *Pira International Conference. Ink on Paper*, January 2003.
13. ISO/IEC 13660.2001 -- Information technology -- Office equipment -- Measurement of image quality attributes for hardcopy output -- Binary monochrome text and graphic images
14. ISO/IEC 15416.2000 -- Information technology -- Automatic identification and data capture techniques -- Bar code print quality test specification -- Linear symbols
15. ISO/IEC 15415.2004 Information technology -- Automatic identification and data capture techniques -- Bar code print quality test specification -- Two-dimensional symbols.
16. ISO/IEC 16022. Information technology – Automatic identification and data capture techniques — Bar code symbology specifications — Data Matrix
17. CEN TS 14826. Postal services – Automatic identification of items - Two dimensional code print quality specification for machine readable Digital Postage Marks. ISO/IEC FCD 18050 Print Quality Attributes for Machine Readable Digital Postage Marks.
18. UPU S28-2 Communication of postal information using two-dimensional symbols
19. UPU S36-4 Digital Postage Marks (DPM) - Applications, security and design
20. UPU S-44-1 Colour and durability attributes of franking marks

Author Biography

Judith Auslander Received her B.Sc. in Chemistry, M. Sc. in Organic Chemistry and Ph. D. in Inorganic Chemistry, all from the Hebrew University in Jerusalem. She joined Pitney Bowes in 1987 where she was responsible for developing ink jet inks for piezo ink jet technology. She also developed fluorescent inks for franking and ink jet, new ink delivery systems based on ink impregnated polymeric foams, and fluorescent thermal transfer ribbons used in Pitney Bowes's first digital postage meter. Most recently, she has studied the mechanism of ink/ paper interactions between ink jet inks and various types of mailing envelopes. For readability of high density bar codes. Dr. Auslander has 22 publications and holds 24 patents in the area of postal inks, bar codes and security inks.